NORDITA – 95/48 P

hep-ph/9506455

Production and Two-photon Decay of the MSSM Scalar Higgs Bosons at the LHC

B. Kileng[a], P. Osland[b], P.N. Pandita[a,c]

[a] NORDITA, Blegdamsvej 17, DK-2100 Copenhagen Ø, Denmark

[b] Department of Physics, University of Bergen, Allégt. 55, N-5007 Bergen, Norway

[c] North Eastern Hill University, Laitumkhrah, Shillong 793003, India*

Abstract

We consider the production and two-photon decay of the CP-even Higgs bosons (h^0 and H^0) of the Minimal Supersymmetric Standard Model (MSSM) at the Large Hadron Collider. We study in detail the dependence of the cross section on various parameters of the MSSM, especially the dependence on the mixing effects in the squark sector due to the Higgs bilinear parameter μ and the soft supersymmetry breaking parameter A. We find that the cross section for the production of these Higgs bosons has a significant dependence on the parameters which determine the chiral mixing in the squark sector. The cross section times the two-photon branching ratio of h^0 is of the order of 15–25 fb in much of the parameter space that remains after imposing the present experimental constraints. For the H^0 the two-photon branching ratio is only significant if the H^0 is light, but then the cross section times the branching ratio may exceed 200 fb. The QCD corrections due to quark loop contributions are known to increase the cross section by 50%. We find the dependence of the cross section on the gluon distribution function used to be rather insignificant.

---

*Permanent address

1 Introduction

It is well known that in the Minimal Supersymmetric Standard Model (MSSM) [1], two Higgs doublets with opposite hypercharge are required in order to preserve supersymmetry. The physical Higgs boson spectrum in the MSSM consists of two CP-even neutral bosons h^0 and H^0, a CP-odd neutral boson A^0 and a pair of charged Higgs bosons $H^{\pm}$. The most important production mechanism for the neutral SUSY Higgs particles at the Large Hadron Collider (LHC) is the gluon fusion mechanism, $pp \to gg \to h^0$, H^0, A^0 [2] and the Higgs radiation off top and bottom quarks [3]. Except for the small range in the parameter space where the heavy neutral Higgs H^0 decays into a pair of Z bosons, the rare $\gamma\gamma$ decay mode, apart from $\tau\tau$ decays, is a promising mode to detect the neutral Higgs particles, especially if b quark decays cannot be separated from the QCD background[1].

This process was studied several years ago [4], and it was concluded that the lightest Higgs could be detected in this mode for sufficiently large values of the mass of the pseudoscalar Higgs boson $m_A \gg m_Z$. Similarly, the $\gamma\gamma$ channel is important for the discovery of H^0 for 50 GeV $\leq m_A \leq$ 150 GeV. Related studies have been presented in ref. [5]. While most of the emphasis in these earlier works was on the SSC, the discussion of the dependence of the cross section on various parameters is relevant.

In this paper we present a fresh study of the hadronic production and subsequent two-photon decay of the CP-even Higgs bosons (h^0 and H^0) of the MSSM, valid for the LHC energy of $\sqrt{s} = 14$ TeV, and using gluon distribution functions based on recent HERA data [6], to reassess the feasibility of observing the CP-even Higgs bosons in this mode. As mentioned earlier, the gluon fusion mechanism is the dominant production mechanism of SUSY Higgs bosons in high-energy pp collisions throughout the entire Higgs mass range. We study the cross section for the production of the h^0 and H^0, and their decays, taking into account all the parameters of the model. In particular, we take into account the mixing in the squark sector, the chiral mixing, which also affects the Higgs boson masses through appreciable radiative corrections. This was previously shown to lead to large corrections

[1]It should be kept in mind that if SUSY particles are light, decays to squarks and charginos, $h^0 \to \tilde{q}\tilde{q}$, $h^0 \to \tilde{\chi}^+\tilde{\chi}^-$, could be seen at LEP2.

to the rates [7].

In the calculation of the production of the Higgs through gluon-gluon fusion, we include in the triangle graph loop all the squarks, as well as b and t quarks, the lightest quarks having a negligible coupling to the h^0. On the other hand, in the calculation of decay of the Higgs to two photons, we include in addition to the above, all the sleptons, $W^{\pm}$, charginos and the charged Higgs boson.

The Minimal Supersymmetric Model contains several soft supersymmetry-breaking terms. We write the relevant soft terms in the Lagrangian as follows [8]

$$\begin{aligned}\mathcal{L}_{\rm Soft} &= \left\{\frac{g m_d A_d}{\sqrt{2}\, m_W \cos\beta} Q^{\rm T}\epsilon H_1 \tilde{d}^R - \frac{g m_u A_u}{\sqrt{2}\, m_W \sin\beta} Q^{\rm T}\epsilon H_2 \tilde{u}^R + \text{h.c.}\right\} \\ &\quad -\widetilde{M}_U^2 Q^\dagger Q - \widetilde{m}_U^2 \tilde{u}^{R\dagger}\tilde{u}^R - \widetilde{m}_D^2 \tilde{d}^{R\dagger}\tilde{d}^R - M_{H_1}^2 H_1^\dagger H_1 - M_{H_2}^2 H_2^\dagger H_2 \\ &\quad + \frac{M_1}{2}\left\{\lambda\lambda + \bar{\lambda}\,\bar{\lambda}\right\} + \frac{M_2}{2}\sum_{k=1}^{3}\left\{\Lambda^k\Lambda^k + \bar{\Lambda}^k\bar{\Lambda}^k\right\}. \end{aligned} \tag{1.1}$$

Subscripts u (or U) and d (or D) refer generically to up and down-type quarks. The Higgs production cross section and the two-photon decay rate depend significantly on several of these parameters.

Even without chiral mixing, two basic mass scales are required, those of squark and gaugino masses. The squark masses are determined by an SU(2)-doublet mass parameter, together with two SU(2)-singlet mass parameters, denoted in eq. (1.1) by $\widetilde{M}_U$, $\widetilde{m}_U$ and $\widetilde{m}_D$, respectively. As is often done, we consider the case when all the SUSY-breaking squark masses are taken equal to a common mass parameter, which we denote by $\widetilde{m}$ ($= \widetilde{M}_U = \widetilde{m}_U = \widetilde{m}_D$). We shall consider the situation where this parameter is chosen to be 150 GeV for the first two generations, and vary it over the values 150, 500 and 1000 GeV for the third generation. (Most of the plots presented will be for $\widetilde{m} = 500$ GeV.) The physical squark masses will in general be different from these values, but they determine the relevant orders of magnitude.

The contributions from the squark and Higgs sectors depend on the relative sign between the A and μ parameters, but not on their overall signs. I.e., we can choose A positive, but then we must study both negative and positive values of μ in order to cover all of parameter space. The Higgs sector depends on A and μ through the radiative corrections.

The contribution from the chargino sector depends on the relative sign between μ and M_2. The chargino contribution is independent of A. Thus, the $h^0 \to \gamma\gamma$ decay rate is independent of the the over-all signs of A, μ and M_2, but depends on all the relative signs. To be more specific, we may choose M_2 positive, but then A and μ must both be allowed to take on negative and positive values in order to cover the full parameter space. In most of the parameter space though, the dependence on the chargino mass (and therefore also on the sign of M_2) is rather weak. In these regions it suffices to consider A positive.

The signs of the off-diagonal terms in the squark mass matrices are given by the definition of A and μ, and also by the definition of the fermion masses. The sign chosen for the fermion mass terms show up in some of the couplings, in the fermion propagators and the spin sums.

Having μ and A non-zero has implications for the Higgs masses as well. These will be presented in Sec. 2, together with constraints related to other masses, before we come to the study of the cross sections and decay rates in Secs. 3 and 4.

2 Constraints on Parameter Space

As discussed in the Introduction, there are various contributions to the production and decay of the lightest Higgs boson at the LHC, and, therefore, it is necessary to have a description of the full parameter space and the theoretical and experimental constraints on it before embarking on the calculation of the cross section and the decay.

At the tree level, the CP-even neutral Higgs mass matrix is controlled by two parameters, which can be chosen to be m_A and $\tan\beta$. However, there are substantial radiative corrections [9] to the neutral Higgs masses which depend on, besides the top quark mass, the supersymmetric trilinear couplings (A_u, A_d), the soft supersymmetry breaking masses ($\widetilde{M}_U$, $\widetilde{m}_U$, $\widetilde{m}_D$, etc.), the bilinear parameter μ in the superpotential, and $\tan\beta$ ($= v_2/v_1$, where v_2 and v_1 are the vacuum expectation values of the two Higgs doublets of MSSM). More recent radiative corrections [10] typically reduce the Higgs mass by 10–20 GeV. However, they are only valid when the squark masses are of the same order

of magnitude, and will therefore not be used in the present study. As long as the "loop particles" are far from threshold for real production, the cross section does not depend very strongly on the exact value of the Higgs mass.

We shall assume that all the trilinear couplings are equal so that

$$A_u = A_d \equiv A, \tag{2.1}$$

and take the top-quark mass to be 176 GeV [11] in our numerical calculations. We vary the parameters which enter the neutral CP-even Higgs mass matrix in the following ranges:

$$\begin{aligned} 50 \text{ GeV} &\leq m_A \leq 1000 \text{ GeV}, \qquad 1.1 \leq \tan\beta \leq 50.0, \\ 50 \text{ GeV} &\leq |\mu| \leq 1000 \text{ GeV}, \qquad 0 \leq A \leq 1000 \text{ GeV}. \end{aligned} \tag{2.2}$$

Parts of the μ-$\tan\beta$ plane must be excluded because of the experimental constraints on the squark, chargino and h^0 masses. For low values of $\widetilde{m}$, the lightest squark tends to be too light (below the most rigorous experimental bound, ~ 44.5 GeV [12]) or even unphysical (mass squared negative). The excluded region of the parameter space is indicated in fig. 1 for $\widetilde{m} = 150$ GeV, $M_2 = 200$ GeV, $m_A = 200$ GeV and two values of the trilinear coupling A.

The allowed region decreases with increasing A, but the dependence on M_2 and m_A is in this region rather weak. In order to have acceptable b-squarks, μ and $\tan\beta$ must lie *inside* of the hyperbola-shaped curves. Similarly, in order to have acceptable t-squarks, the corners at large $|\mu|$ and small $\tan\beta$ must be excluded.

The chargino masses are, at the tree level, given by the expression

$$\begin{aligned} m^2_{\chi^\pm} &= \frac{1}{2}(M_2^2 + \mu^2) + m_W^2 \\ &\quad \pm \left[\frac{1}{4}(M_2^2 - \mu^2)^2 + m_W^4 \cos^2 2\beta + m_W^2(M_2^2 + \mu^2 + 2\mu M_2 \sin 2\beta)\right]^{1/2} \end{aligned} \tag{2.3}$$

For $\mu = 0$, the above expression simplifies to:

$$m^2_{\chi^\pm} = \frac{1}{2}M_2^2 + m_W^2 \pm \left[\frac{1}{4}M_2^4 + m_W^2 \cos^2 2\beta + m_W^2 M_2^2\right]^{1/2} \tag{2.4}$$

For the case of $\mu = 0$, we see that, for $\tan\beta \gg 1$, the lightest chargino becomes massless. Actually, small values of μ are unacceptable for all values of $\tan\beta$. The lower acceptable

value for $|\mu|$ will depend on $\tan\beta$, but that dependence is rather weak. The region that is excluded due to the chargino being too light, increases with decreasing values of M_2. We note that the radiative corrections to the chargino masses are small for most of the parameter space [13]. We show in fig. 1 the contours in the μ-$\tan\beta$ plane outside of which the chargino has an acceptable mass (> 45 GeV) [14]. By the time the LHC starts operating, one would have searched for charginos with masses up to 90 GeV at LEP2. Contours relevant for LEP2 are also shown.

For larger values of $\widetilde{m}$, there is no problem with squark masses. However, then the radiative corrections to the Higgs masses get large, and correspondingly some regions of parameter space have to be excluded. This is illustrated in fig. 2, for $\widetilde{m} = 500$ GeV. The corners at large values of $|\mu|$ and $\tan\beta$ must be excluded since the h^0 mass there would fall below the experimental bound obtained at LEP [15]. The extent of these forbidden corners grows rapidly as m_A decreases below $\mathcal{O}(150\ \text{GeV})$. They also increase with increasing values of A.

The charged Higgs boson mass is given by

$$m_{H^\pm}^2 = m_W^2 + m_A^2 + \Delta \tag{2.5}$$

where Δ arises due to radiative corrections and is a complicated function of the parameters of the model [16].

The radiative corrections to the charged Higgs mass are not, in general, as large as in the case of neutral Higgs bosons. This is due to an approximate global $SU(2) \times SU(2)$ symmetry [17], valid in the limit of no mixing. In certain regions of parameter space the radiative corrections can, however, be large. This is the case when the trilinear mixing parameter A is large, m_A is small, and when furthermore $\tan\beta$ is large. We shall include the effects of non-zero A and μ in the calculation of the charged Higgs mass. The present experimental limit of order 40–45 GeV [18] is not relevant, but presumably by the time the LHC starts operating, one will at LEP2 have searched for charged Higgs bosons with mass up to around 90 GeV. Even this bound does not appreciably restrict the parameter space as given in figs. 1 and 2.

The neutralino mass matrix depends on four parameters. These are M_2, M_1, μ and

$\tan\beta$. However, one can reduce the number of parameters by assuming that the MSSM is embedded in a grand unified theory so that the SUSY-breaking gaugino masses are equal to a common mass at the grand unified scale. At the electroweak scale, we then have [19]

$$M_1 = \frac{5}{3}\tan^2\theta_{\rm W}\, M_2 \tag{2.6}$$

We shall assume this relation throughout in what follows. The neutralino masses enter the calculation through the total width of the Higgs boson. For the gaugino masses, we take M_2 to be 50, 200, or 1000 GeV. (Most plots will be for $M_2 = 200$ GeV.) The experimental constraint on the lightest neutralino mass rules out certain regions of the parameter space [20], but these depend on several parameters, and are therefore not reproduced in figs. 1 and 2. They are generally correlated with the bounds on chargino masses [14].

3 The lighter CP-even Higgs boson h^0

Let us first consider the cross section for

$$pp \to h^0 X \tag{3.1}$$

For $M_2 = 200$ GeV, $\widetilde{m} = 500$ GeV, and $\mu = 500$ GeV, we show in fig. 3 this cross section for four values of A, the trilinear coupling parameter. The following features are rather striking:

- The cross section decreases appreciably for large values of A. This is mainly due to an increase in the h^0 mass.

- There are sharp edges at small values of $\tan\beta$, and also at small m_A. The edges at small $\tan\beta$ are caused by the h^0 becoming light. At small values of m_A and large A, the couplings of h^0 to b quarks and τ leptons become large, making the cross section very large in this region.

For the same parameters as above, we show in fig. 4 the total decay rate, $\Gamma(h^0 \to \text{all})$ and the two-photon decay rate, $\Gamma(h^0 \to \gamma\gamma)$. As opposed to fig. 3, here we only consider

two values of A, namely $A = 0$ and $A = 1000$ GeV. The two-photon decay rate is seen to increase sharply at large values of A, but this does not result in a larger rate for the process

$$pp \to h^0 X \to \gamma\gamma X \tag{3.2}$$

since the production cross section also decreases, as shown in fig. 3 (mostly due to an increase in the Higgs mass, m_{h^0}). In fig. 5 we show the cross section for the process (3.2). A characteristic feature of the cross section is that it is small at moderate values of m_A, and then increases steadily with increasing m_A, reaching asymptotically a plateau. This behaviour is caused by the contribution of the W to the triangle graph for $h^0 \to \gamma\gamma$. The h^0WW coupling is proportional to $\sin(\beta - \alpha)$, where α is defined in terms of masses (including radiative corrections) as

$$\cos 2\alpha = -\cos 2\beta \left(\frac{m_A^2 - m_Z^2}{m_{H^0}^2 - m_{h^0}^2} \right), \qquad -\frac{\pi}{2} \leq \alpha \leq 0. \tag{3.3}$$

For large m_A, at fixed β, all Higgs masses, except m_{h^0}, become large, so that h^0 decouples. For large m_A, we actually have $\sin(\beta - \alpha) \to 1$, which is why the cross section increases and reaches a plateau for large m_A.

In figures 6 and 7 we show contour plots of the cross section (3.2), for $M_2 = 200$ GeV, $\widetilde{m} = 500$ GeV and μ equal to -500 and $+500$ GeV, respectively. For each case, four values of the trilinear chiral-mixing parameter A are considered, $A = 0$, 200 GeV, 500 GeV and 1000 GeV (figure 7a is thus a different representation of figure 5).

The μ-dependence of the cross section can for the case of $M_2 = 200$ GeV and $\widetilde{m} = 500$ GeV be described as follows. At moderate values ($\mu = \pm 200$ GeV), there is not much difference between the cross section for positive and negative values of μ. The cross section has a significant dependence on m_A, being low at $m_A \leq \mathcal{O}(300$ GeV), then increasing steadily and reaching a plateau with increasing m_A. The dependence on $\tan\beta$ is rather weak.

For increasing values of $|\mu|$ (500 GeV, 1000 GeV) the change in the cross section is rather complex. This is basically caused by two phenomena: (1) At large values of $|\mu|$ the squarks become too light or unphysical, in analogy with the case ($M_2 = 200$ GeV, $\widetilde{m} = 150$ GeV) shown in fig. 1. Hence, there are regions both at small and large values of

$\tan\beta$ where the cross section is not defined. (2) At large values of $|\mu|$ and large values of $\tan\beta$ (all m_A) the Higgs gets very light (due to radiative corrections). As a consequence, the cross section can get rather high, where not forbidden due to (1) above.

The dependence of the cross section on M_2 and $\widetilde{m}$ is described in table 1. For small values of $\widetilde{m}$ (~ 150 GeV), the possible ranges of $\tan\beta$, μ and A become severely restricted, in order to obtain physically acceptable squark masses. There is a significant increase in the cross section as $\widetilde{m}$ increases from 500 GeV to 1 TeV, to values of the order of 25–30 fb.

For small values of M_2 (~ 50 GeV), the possible range in μ is restricted in order to obtain physically acceptable chargino masses. As M_2 increases beyond 200 GeV, there is little further change in the cross section. Details are given in table 1.

The cross section has a modest dependence on the choice of gluon distribution function used. For the plots shown here, we have used the recent GRV Set 3 [21] distributions, which are the default of the PDFLIB. The BM Set 1 [22] leads to an increase of the cross section by about 5–6%, whereas the MRS Set 29 (S0') [23] and CTEQ Set 24 (2pM) [24] give reductions by 3–5% and 8–9%, respectively. These uncertainties are thus rather insignificant.

4 The heavier CP-even Higgs boson H^0

We shall here briefly consider the process

$$pp \to H^0 X \to \gamma\gamma X \tag{4.1}$$

which is of interest for small values of m_A.

The two-photon decay of the heavier CP-even Higgs proceeds dominantly through W loops, and is complementary to that of the lighter CP-even Higgs. It is only significant if m_A is small, hence m_{H^0} itself must also be light. At small m_A the total H^0 decay rate is small and thus the branching ratio for it to go into two photons can be considerable. As a result, the cross section for the process (4.1) can at small values of m_A reach values exceeding 200 fb.

Contour plots of the cross section are shown in figures 8 and 9, for four values of A, and for $\mu = -500$ GeV (fig. 8) and $\mu = 500$ GeV (fig. 9). For $\mu = -500$ GeV there is a strong *increase* in the cross section with increasing values of A. For positive values of μ, however, increasing values of A lead to a reduction of the cross section. At low values of m_A the Higgs mass m_{H^0} is of the order of 110–140 GeV, and the h^0 mass is close to the experimental lower limit.

5 Summary and concluding remarks

We have discussed in some detail the cross section for producing the CP-even Higgs bosons at the LHC, in conjunction with their decay to two photons. Where the parameters lead to a physically acceptable phenomenology, the cross section multiplied by the two-photon branching ratio is for the lighter CP-even Higgs boson of the order of 20–30 fb.

These numbers do not take into account QCD corrections. Such corrections have been evaluated for the quark-loop contribution, and lead to enhancements of the cross section of about 50% [25]. However, in the presence of chiral mixing the squark loops also contribute significantly. Since the QCD corrections for these are not available, we have decided it was more clean to simply leave out all higher-order QCD effects. One should of course keep in mind that they are very important.

There is a modest increase of the cross section with increasing values of A (i.e., with increasing chiral mixing). This comes about as the result of two competing effects: with increasing A, the Higgs boson becomes more heavy, leading to lower production cross sections. This is however offset by a corresponding increase in the two-photon decay rate.

This research has been supported by the Research Council of Norway. The work of PNP was supported by the Department of Science and Technology under project No. SP/S2/K-17/94. One of the authors (PNP) would like to thank NORDITA and the University of Bergen for hospitality while this work was done. We are also grateful to P. Janot, P. Zerwas and F. Zwirner for useful correspondence and interest in this work.

References

[1] H.-P. Nilles, Phys. Rep. C110 (1984) 1;
H. E. Haber and G. L. Kane, Phys. Rep. C117 (1985) 75;
R. Barbieri, Riv. Nuovo Cimento 11 (1988) No. 4, p. 1;
For a recent review, see, e.g., R. Arnowitt and P. Nath, Lecture at Swieca School, Campos do Jordao, Brazil, 1993; in *Sao Paulo 1993*, Proceedings, Particles and fields, 3-63; CTP-TAMU-93-052 and NUB-TH-3073-93, hep-ph/9309277.

[2] H. M. Georgi, S. L. Glashow, M. E. Machacek, and D. V. Nanopoulos, Phys. Rev. Lett. 40 (1978) 692.

[3] Z. Kunszt, Nucl. Phys. B247 (1984) 339;
W.J. Marciano and F.E. Paige, Phys. Rev. Lett. 66 (1991) 2433;
J.F. Gunion, Phys. Lett. B261 (1991) 510.

[4] Z. Kunszt and F. Zwirner, Nucl. Phys. B385 (1992) 3.

[5] H. Baer, M. Bisset, C. Kao and X. Tata, Phys. Rev. D46 (1992) 1067;
V. Barger, M.S. Berger, A.L. Stange and R.J.N. Phillips, Phys. Rev. D45 (1992) 4128;
J.F. Gunion and L.K. Orr, Phys. Rev. D46 (1992) 2052;
V. Barger, Kingman Cheung, R.J.N. Phillips and A.L. Stange, Phys. Rev. D46 (1992) 4914.

[6] H. Plothow-Besch, PDFLIB (CERNLIB), version 4.17; Comp. Phys. Comm. 75 (1993) 396.

[7] B. Kileng, Zeitschrift f. Physik, C63 (1994) 87.

[8] L. Girardello and M.T. Grisaru, Nucl. Phys. B194 (1982) 65; see also ref. [7].

[9] Y. Okada, M. Yamaguchi, T. Yanagida, Prog. Theor. Phys. 85 (1991) 1; Phys. Lett. B262 (1991) 54;
J. Ellis, G. Ridolfi and F. Zwirner, Phys. Lett. B257 (1991) 83; Phys. Lett. B262

(1991) 477;
H.E. Haber and R. Hempfling, Phys. Rev. Lett. 66 (1991) 1815.

[10] M. Carena, J.R. Espinosa, M. Quiros and C.E.M. Wagner, CERN-preprint CERN-TH/95-45, hep-ph/9504316.

[11] CDF Collaboration, F. Abe, et al., Phys. Rev. Lett. 73 (1994) 225;
CDF Collaboration, F. Abe, et al., FERMILAB-PUB-95-022-E, hep-ex/9503002;
D0 Collaboration, S. Abachi, et al., FERMILAB-PUB-95-028-E, hep-ex/9503003.

[12] DELPHI Collaboration, P. Abreu et al., Phys. Lett. B247 (1990) 148;
OPAL Collaboration, R. Akers et al., Phys. Lett. B337 (1994) 207.

[13] D. Pierce and A. Papadopoulos, Phys. Rev. D50 (1994) 565; Nucl. Phys. B430 (1994) 278;
A.B. Lahanas, K. Tamvakis and N.D. Tracas, Phys. Lett. B324 (1994) 387.

[14] ALEPH Collaboration, D. Decamp, et al., Phys. Lett. B236 (1990) 86.

[15] ALEPH Collaboration, D. Buskulic, et al., Phys. Lett. B313 (1993) 312.

[16] A. Brignole, J. Ellis, G. Ridolfi and F. Zwirner, Phys. Lett. B271 (1991) 123;
A. Brignole, Phys. Lett. B277 (1992) 313;
M.A. Diaz and H.E. Haber, Phys. Rev. D45 (1992) 4246.

[17] H.E. Haber and A. Pomarol, Phys. Lett. B302 (1993) 435.

[18] ALEPH Collaboration, D. Buskulic, et al., Phys. Lett. B241 (1990) 623.

[19] K. Inoue, A. Kakuto, H. Komatsu, S.Takeshita, Prog. Theor. Phys. 68(1982) 927, Erratum *ibid.* 70 (1983) 330; *ibid.* 71 (1984) 413.

[20] R. Barbieri, G. Gamberini, G.F. Giudice and G. Ridolfi, Phys. Lett. 195B (1987) 500;
J. Ellis, G. Ridolfi and F. Zwirner, Phys. Lett. 237B (1990) 423.

[21] M. Glück, E. Reya and A. Vogt Z. Phys. C53 (1992) 127.

[22] E.L. Berger and R. Meng, Phys. Lett. 304B (1993) 318; CERN-TH 6739/92; ANL-HEP-CP-92-108 and E.L. Berger, R. Meng and J. Qiu, ANL-HEP-CP-92-79.

[23] A.D. Martin, R.G. Roberts and W.J. Stirling, Phys. Lett. 306B (1993) 145 and Phys. Lett. 309B (1993) 492.

[24] J. Botts et al., Phys. Lett. 304B (1993) 159.

[25] M. Spira, A. Djouadi, D. Graudenz and P.M. Zerwas, DESY 94-123, hep-ph/9504378.

Table 1. Dependence of the cross section for $pp \to h^0 X \to \gamma\gamma X$ on M_2, $\widetilde{m}$ and μ

M_2	$\widetilde{m} = 150$ GeV lightest squark too light for large values of $\tan\beta$ and increasing A	$\widetilde{m} = 500$ GeV	$\widetilde{m} = 1000$ GeV
50 GeV lightest chargino too light for small values of $\tan\beta$ and positive μ	cross section significant only for small A, small $\tan\beta$, and small negative μ	cross section lower than at $M_2 = 200$ GeV, especially at moderate, positive μ; for large $\lvert\mu\rvert$ cross section significant only for narrow range in $\tan\beta$	cross section larger than at $\widetilde{m} = 500$ GeV
200 GeV	cross section significant only for small A, small $\tan\beta$, and small $\lvert\mu\rvert$	"default" given in figs. 3–9 for $\mu = \pm 500$ GeV; complex dependence on $\tan\beta$ for larger $\lvert\mu\rvert$	cross section significantly *larger* than at $\widetilde{m} = 500$ GeV, reaching well beyond 25 fb for large range of μ; less dependence on $\tan\beta$ than at $\widetilde{m} = 500$ GeV, in particular for large A
500 GeV 1000 GeV	very similar to $M_2 = 200$ GeV	very similar to $M_2 = 200$ GeV	very similar to $M_2 = 200$ GeV

Figure captions

Fig. 1. Regions in the μ-$\tan\beta$ plane which are ruled out by too light chargino ($\chi^\pm$) and squark masses. The gaugino mass scale is $M_2 = 200$ GeV, $\widetilde{m} = 150$ GeV, and $m_A = 200$ GeV. At this low value of $\widetilde{m}$, the squark masses are too light or unphysical in much of the μ-$\tan\beta$ plane. The hyperbola-like contours give regions that are excluded by the lightest b squark being below 45 GeV (solid) or 90 GeV (dashed). The more straight contours at large μ and small $\tan\beta$ similarly indicate regions that are excluded by the lightest t squark. In a) we consider the trilinear mixing parameter $A = 0$, whereas in b) we take $A = 200$ GeV.

Fig. 2. Regions in the μ-$\tan\beta$ plane which are ruled out by too light chargino ($\chi^\pm$) and h^0 masses. Similar to fig. 1, but for $\widetilde{m} = 500$ GeV. In a) we consider the trilinear mixing parameter $A = 0$, whereas in b) we take $A = 1000$ GeV. The solid (dashed) contours for small $|\mu|$ refer to the chargino mass $m_{\chi^\pm} = 45$ (90) GeV. The unlabelled contours near the corners at large $|\mu|$ refer to regions where the h^0 mass would be below 45 GeV.

Fig. 3. Cross section for $pp \to h^0 X$ as a function of m_A and $\tan\beta$ for $M_2 = 200$ GeV, $\widetilde{m} = 500$ GeV, and $\mu = 500$ GeV. Four values of A are considered: a) $A = 0$, b) $A = 200$ GeV, c) $A = 500$ GeV and d) $A = 1000$ GeV.

Fig. 4. Total decay rate $\Gamma(h^0 \to \text{all})$ and two-photon decay rate $\Gamma(h^0 \to \gamma\gamma)$, as functions of m_A and $\tan\beta$ for $M_2 = 200$ GeV, $\widetilde{m} = 500$ GeV, and $\mu = 500$ GeV. Two values of A are considered: $A = 0$ and $A = 1000$ GeV.

Fig. 5. Cross section for $pp \to h^0 X \to \gamma\gamma X$ as a function of m_A and $\tan\beta$ for $M_2 = 200$ GeV, $\widetilde{m} = 500$ GeV, $\mu = 500$ GeV, and $A = 0$.

Fig. 6. Dependence of the $pp \to h^0 \to \gamma\gamma$ cross section on m_A and $\tan\beta$ for different values of the trilinear couplings A. Four values of A are considered: a) $A = 0$, b) $A = 200$ GeV, c) $A = 500$ GeV and d) $A = 1000$ GeV. Here $M_2 = 200$ GeV, $\widetilde{m} = 500$ GeV, and $\mu = -500$ GeV. The solid contours are at 15 fb, the long-dashed ones at 20 fb, and the short-dashed ones at 25 fb.

Fig. 7. Dependence of the $pp \to h^0 \to \gamma\gamma$ cross section on m_A and $\tan\beta$ for different

values of the trilinear couplings A. As fig. 6, except that $\mu = 500$ GeV.

Fig. 8. Dependence of the $pp \to H^0 \to \gamma\gamma$ cross section on m_A and $\tan\beta$ for different values of the trilinear couplings A. Four values of A are considered: a) $A = 0$, b) $A = 200$ GeV, c) $A = 500$ GeV and d) $A = 1000$ GeV. Here $M_2 = 200$ GeV, $\widetilde{m} = 500$ GeV, and $\mu = -500$ GeV. The contours are at 10 fb (solid), 20 fb, 50 fb, 100 fb and 200 fb.

Fig. 9. Dependence of the $pp \to H^0 \to \gamma\gamma$ cross section on m_A and $\tan\beta$ for different values of the trilinear couplings A. As in fig. 8, except that $\mu = 500$ GeV.

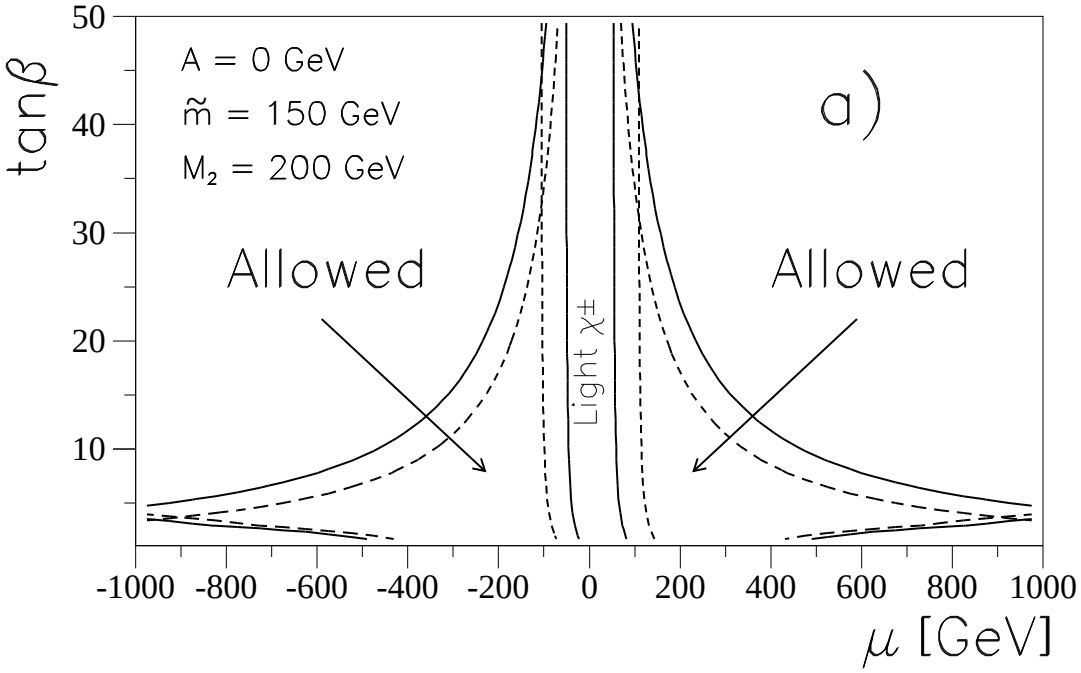
tanβ
A = 0 GeV
m̃ = 150 GeV
M₂ = 200 GeV
a)
Allowed
Allowed
Light χ±
50
40
30
20
10
-1000 -800 -600 -400 -200 0 200 400 600 800 1000
μ [GeV]

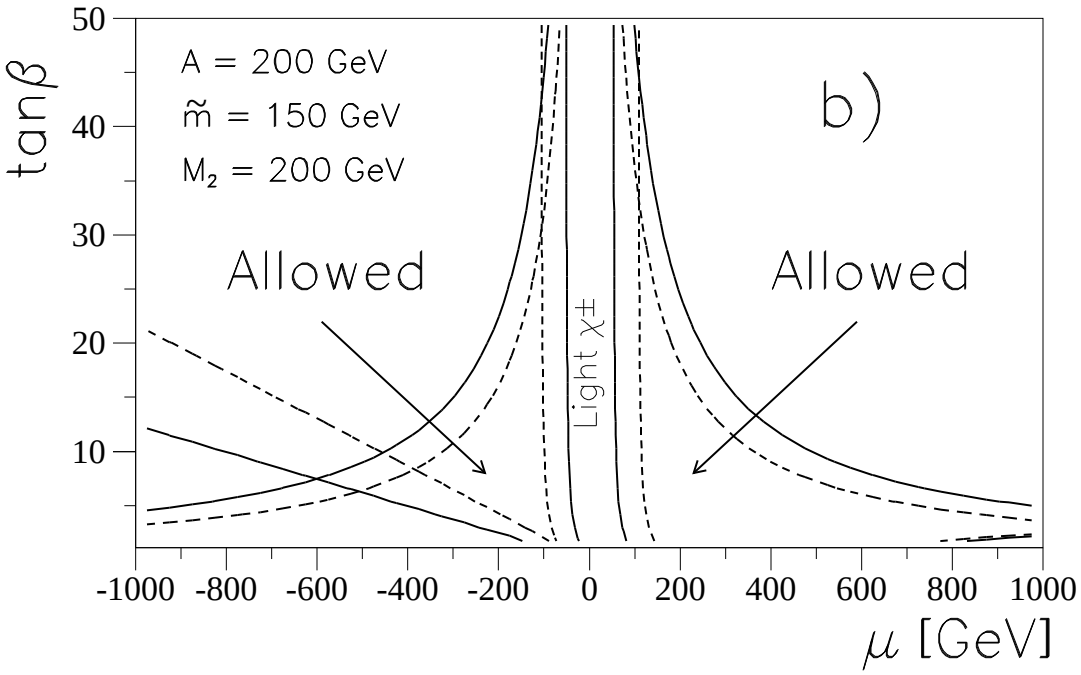
tanβ
A = 200 GeV
m̃ = 150 GeV
M₂ = 200 GeV
b)
Allowed
Allowed
Light χ±
50
40
30
20
10
-1000 -800 -600 -400 -200 0 200 400 600 800 1000
μ [GeV]

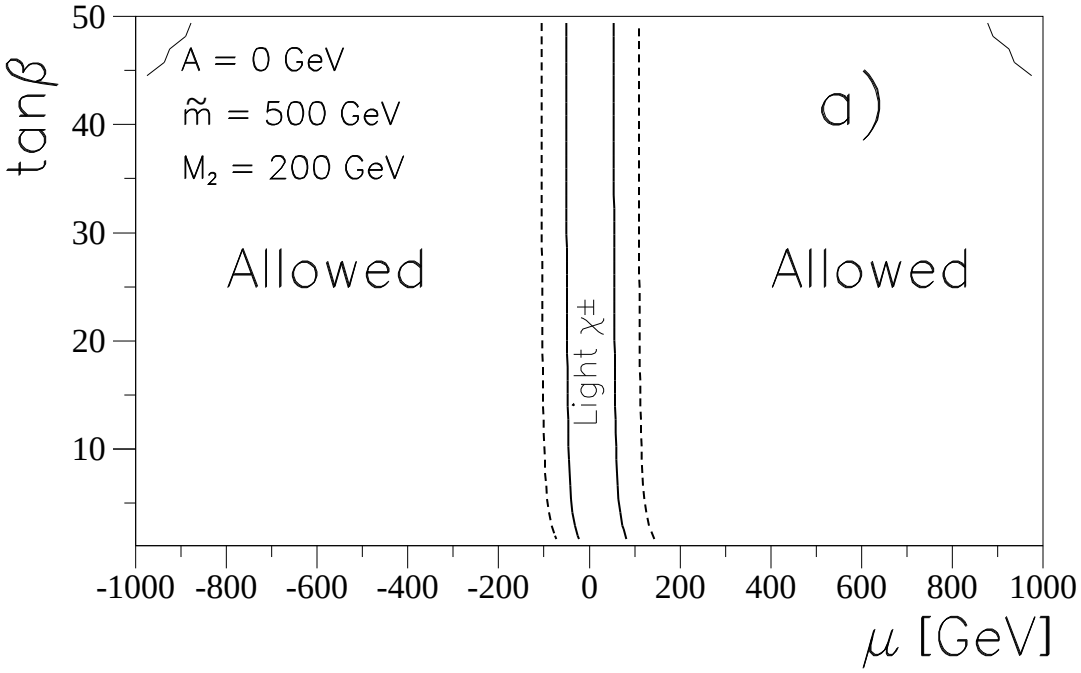
A = 0 GeV
m̃ = 500 GeV
M₂ = 200 GeV
a)
Allowed
Allowed
Light χ±
tanβ
50
40
30
20
10
-1000 -800 -600 -400 -200 0 200 400 600 800 1000
μ [GeV]

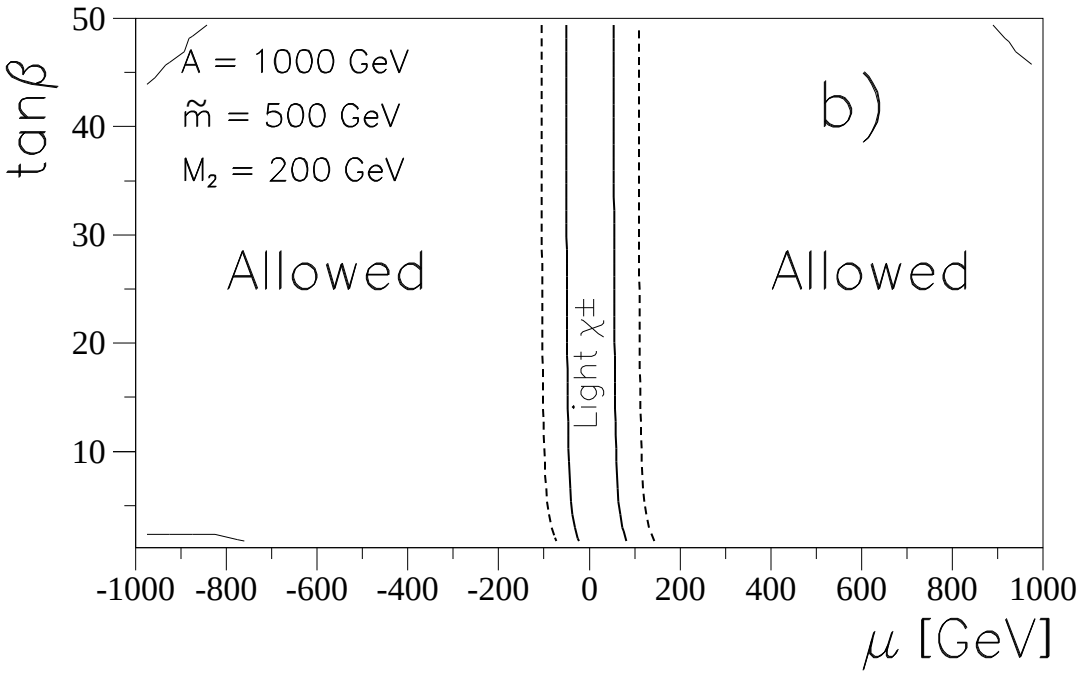
A = 1000 GeV
m̃ = 500 GeV
M₂ = 200 GeV
b)
Allowed
Allowed
Light χ±
tanβ
50
40
30
20
10
-1000 -800 -600 -400 -200 0 200 400 600 800 1000
μ [GeV]

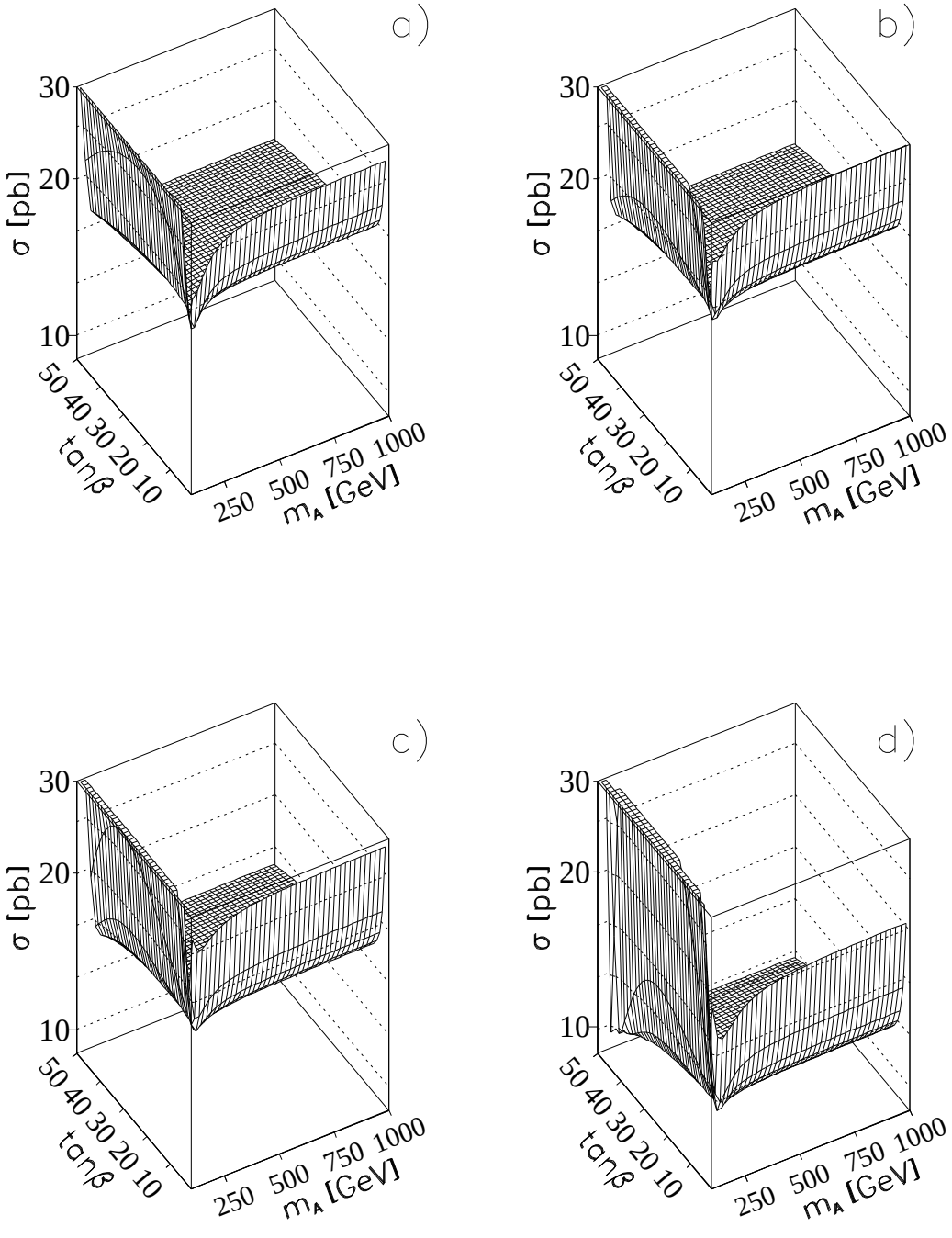
a)
b)
c)
d)
σ [pb]
30
20
10
50 40 30 20 10
tanβ
250 500 750 1000
m_A [GeV]

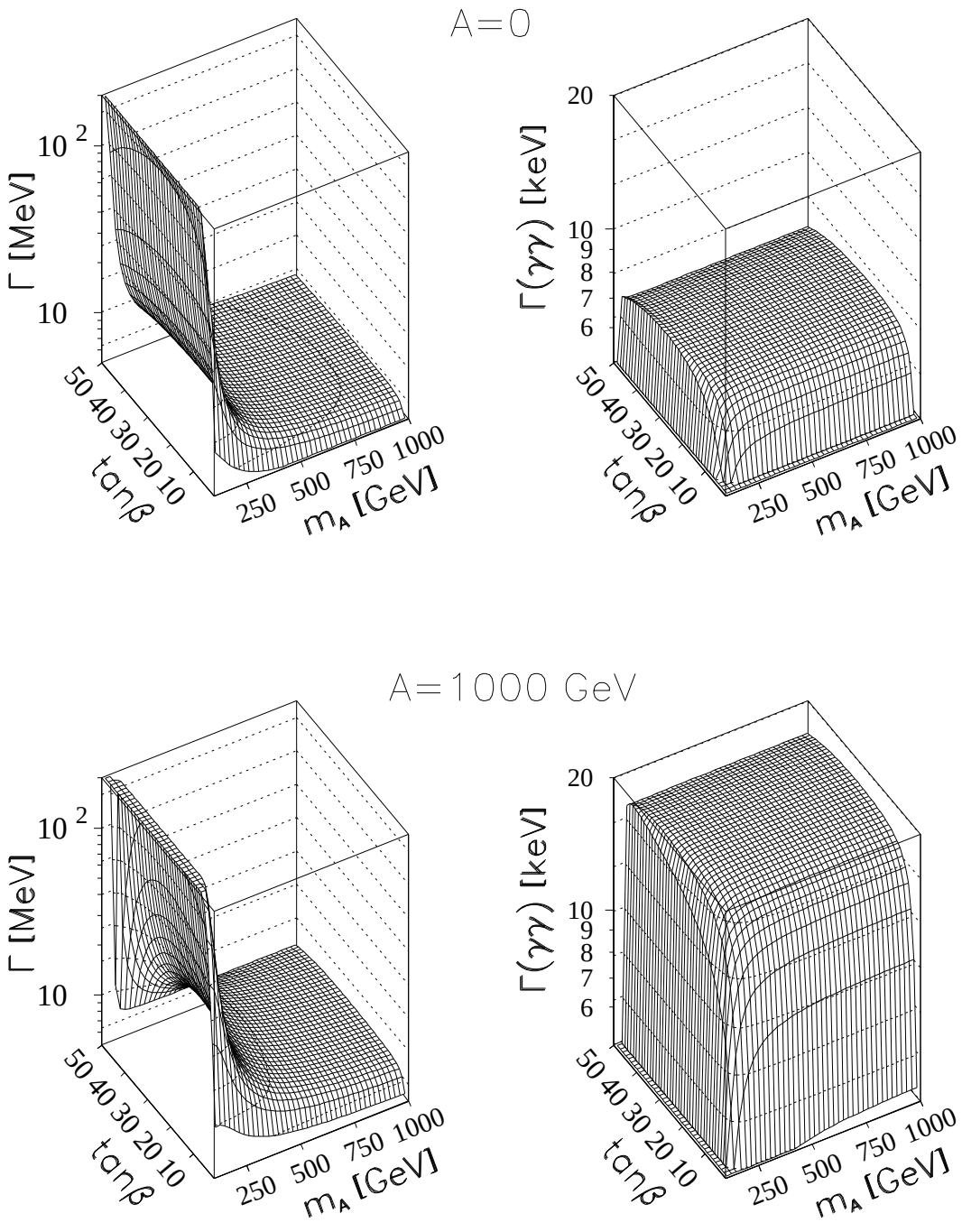
A=0
Γ [MeV]
10 2
10
50 40 30 20 10
tanβ
250 500 750 1000
m_A [GeV]
Γ(γγ) [keV]
20
10
9
8
7
6
50 40 30 20 10
tanβ
250 500 750 1000
m_A [GeV]
A=1000 GeV
Γ [MeV]
10 2
10
50 40 30 20 10
tanβ
250 500 750 1000
m_A [GeV]
Γ(γγ) [keV]
20
10
9
8
7
6
50 40 30 20 10
tanβ
250 500 750 1000
m_A [GeV]

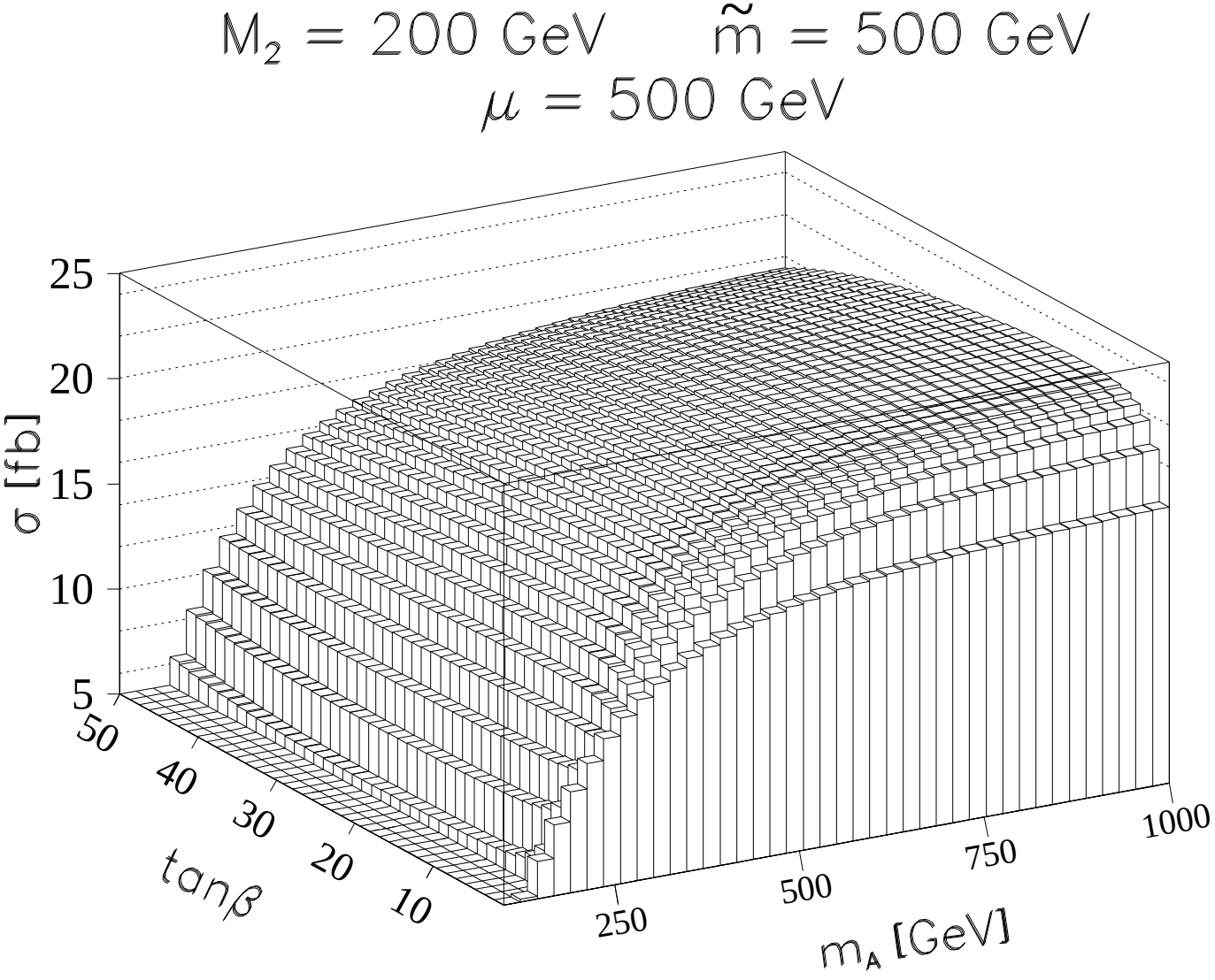
$M_2 = 200$ GeV $\quad \tilde{m} = 500$ GeV
$\mu = 500$ GeV
σ [fb]
25
20
15
10
5
50
40
30
20
10
tanβ
250
500
750
1000
m_A [GeV]

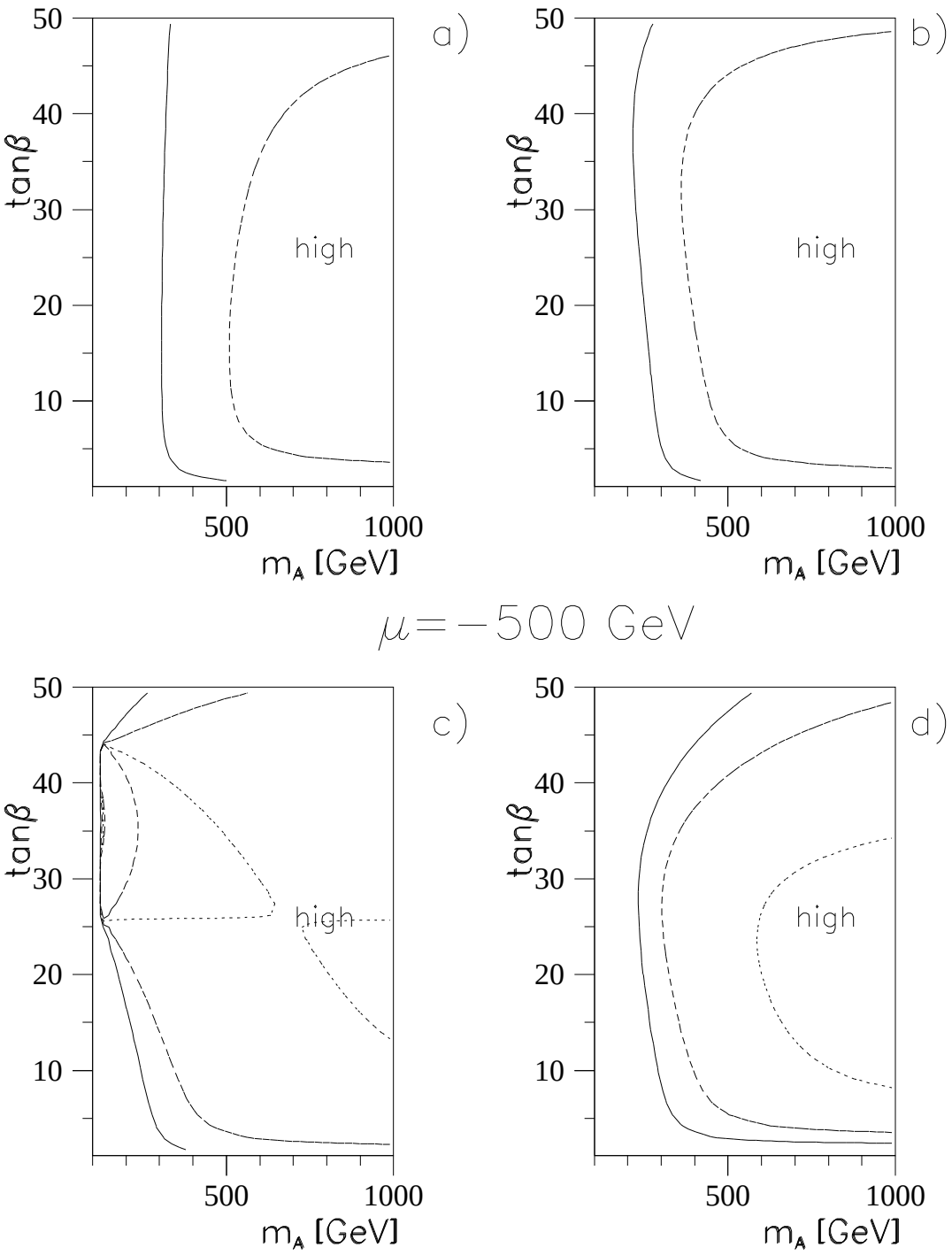
a)
b)
c)
d)
high
tanβ
m_A [GeV]
50
40
30
20
10
500
1000
μ = −500 GeV

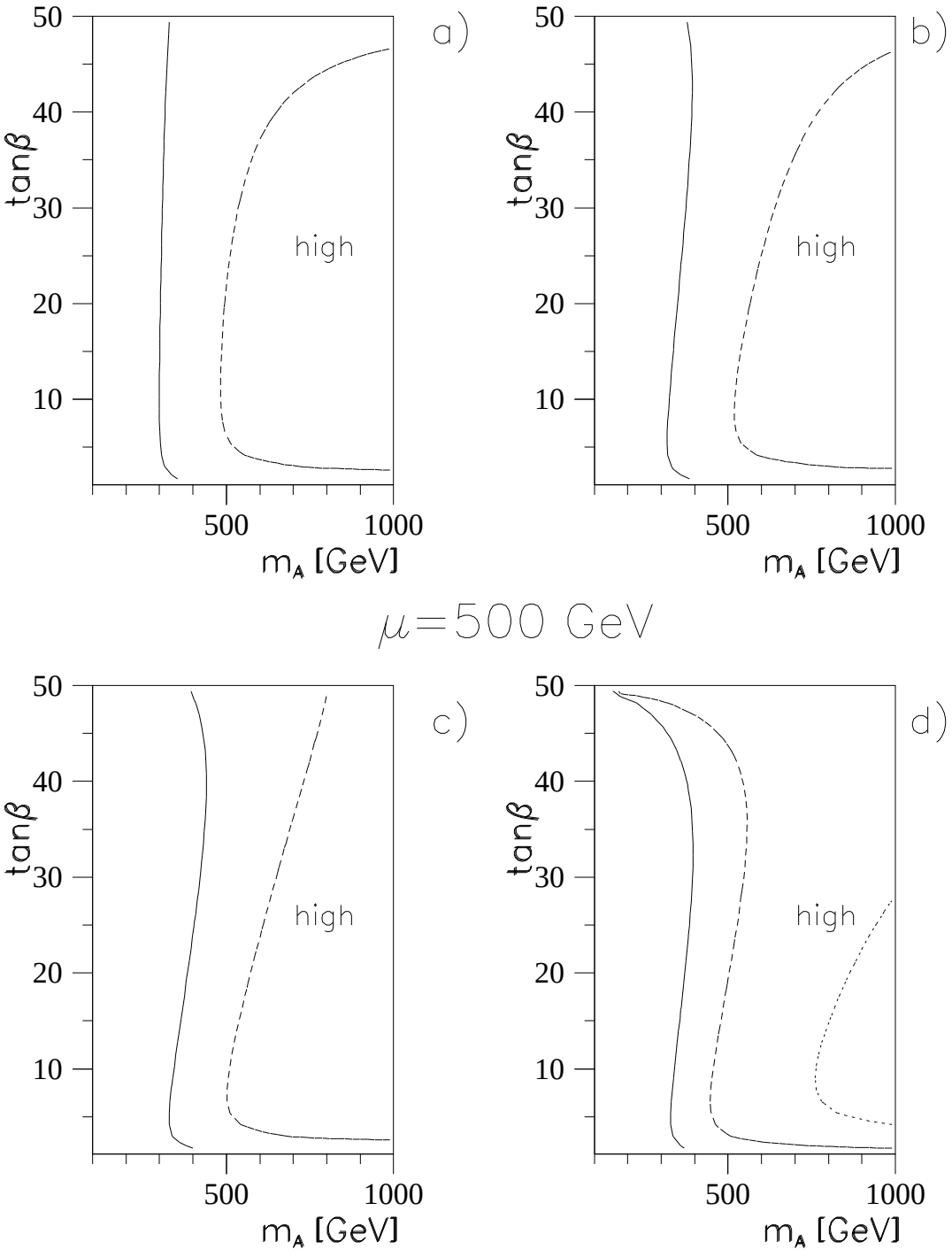
a)
b)
c)
d)
high
tanβ
m_A [GeV]
500
1000
10
20
30
40
50
μ=500 GeV

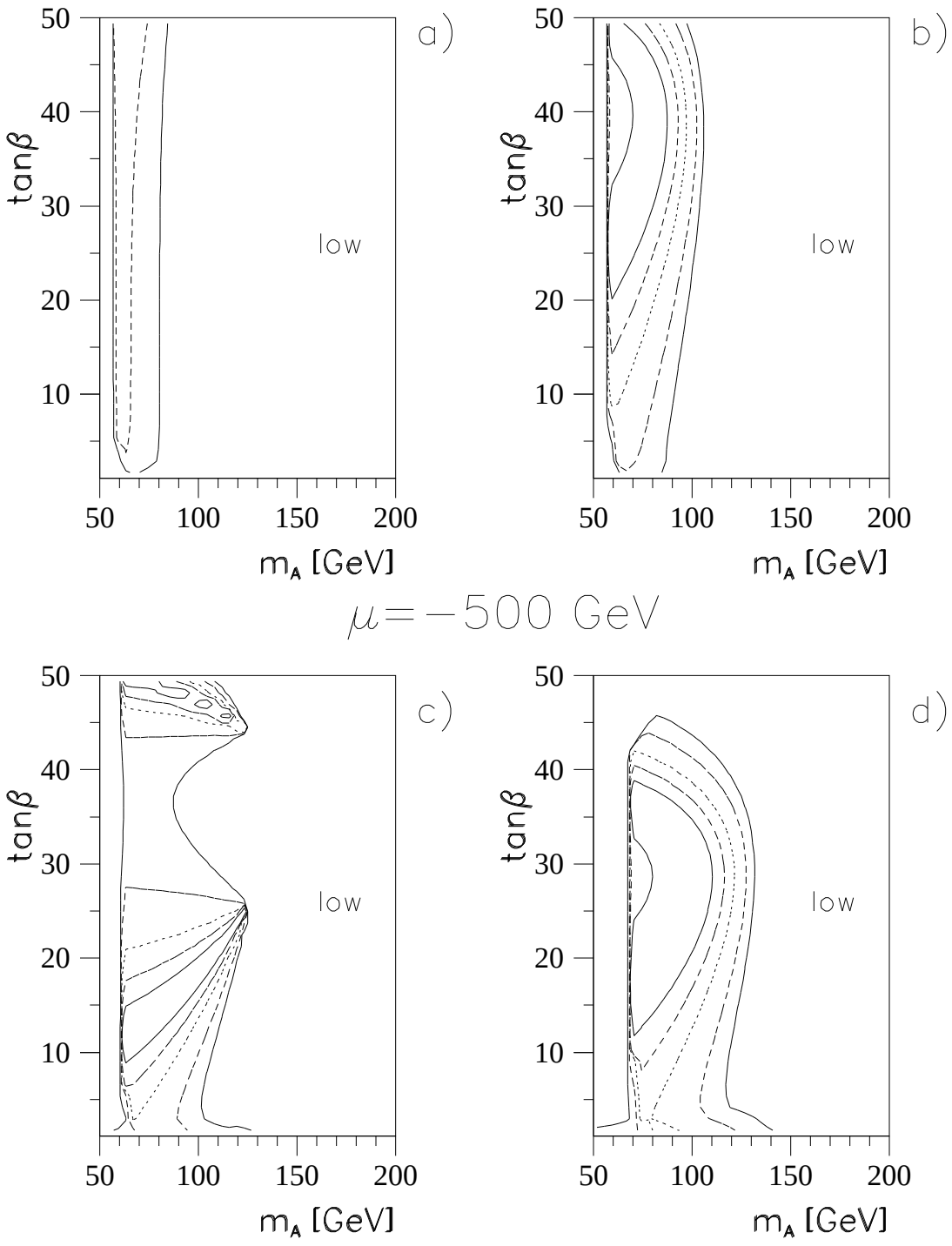
a)
b)
c)
d)
low
tanβ
m_A [GeV]
50
40
30
20
10
50
100
150
200
μ = −500 GeV

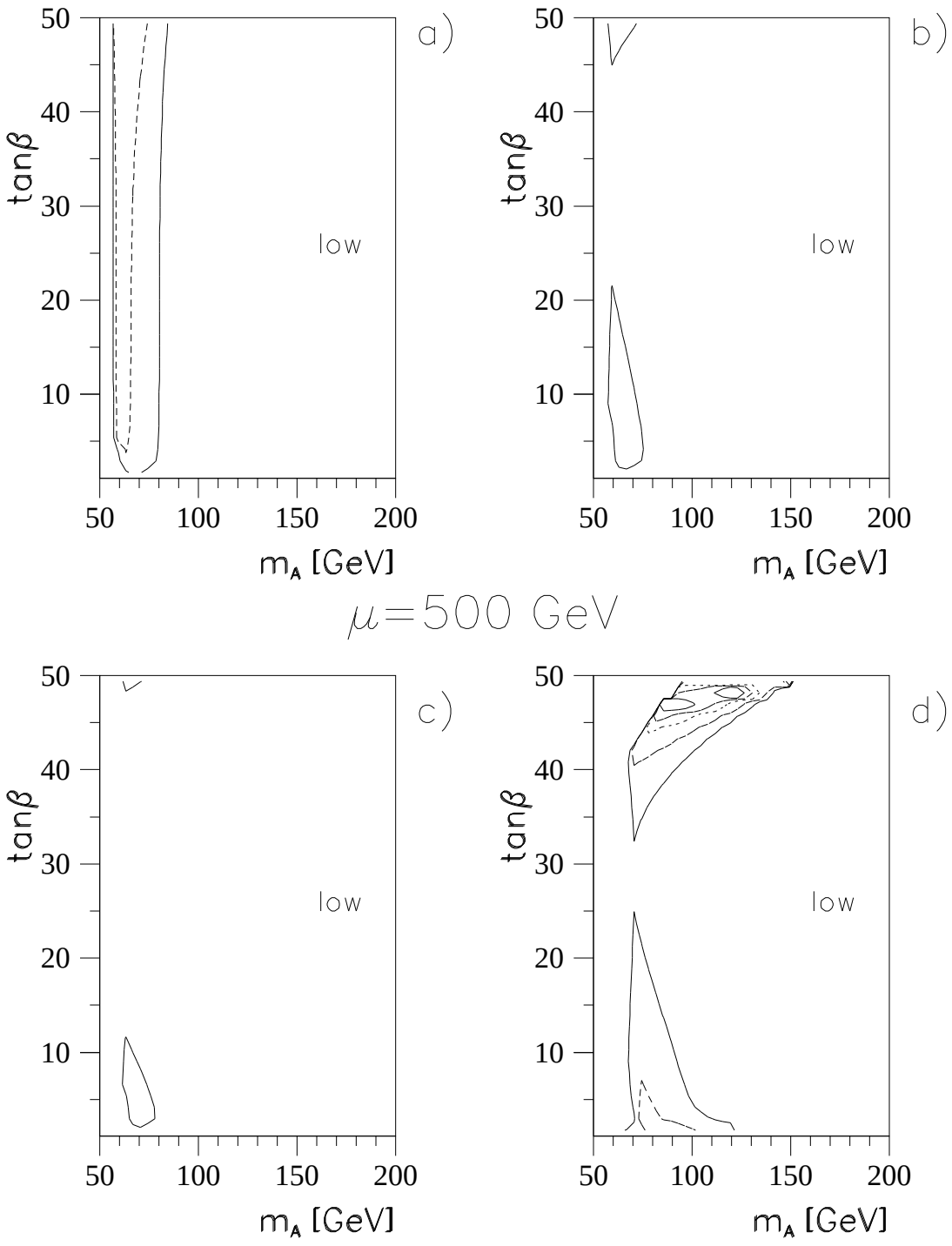
a)
b)
c)
d)
low
tanβ
m_A [GeV]
50
40
30
20
10
50
100
150
200
μ=500 GeV